

Jefferson Lab PAC 47 Jeopardy

**Update on**  
**E12-06-101: Measurement of the Charged Pion Form Factor to High  $Q^2$**   
**and**  
**E12-07-105: Scaling Study of the L–T Separated Pion Electroproduction**  
**Cross Section at 11 GeV**

June 7, 2019

We present an update, and optimized and linked run-plan for our two approved experiments, E12-06-101 and E12-07-105, that allows for the measurement of the pion form factor at the highest  $Q^2$  achievable at a 12 GeV Jefferson Lab, and provides valuable exclusive  $\pi^+$  production data over a large kinematic range, needed for the reliable interpretation of the results of the JLab GPD program. Please refer to the E12-06-101 [1] and E12-07-105 [2] proposals for full details on scientific justification, experimental method and projected uncertainties.

D. Gaskell

*Physics Division, TJNAF, Newport News, VA*

T.Horn (Contact: E12-07-105)

*Catholic University of America, Washington, DC*

*Physics Division, TJNAF, Newport News, VA*

G.M. Huber (Contact: E12-06-101)

*University of Regina, Regina, SK, Canada*

## I. BACKGROUND

The pion occupies a special role in nature [3]. It is the lightest quark system, with a single valence quark and a single valence antiquark. It is also the particle responsible for the long-range character of the strong interaction that binds the atomic nucleus together. A general belief is that the rules governing the strong interaction are left-right, *i.e.* chirally, symmetric. If this were true, the pion would have no mass. The chiral symmetry of massless QCD is broken dynamically by quark-gluon interactions and explicitly by inclusion of light quark masses, giving the pion mass. The pion is thus seen as the key to confirm the mechanism that dynamically generates nearly all of the mass of hadrons and central to the effort to understand hadron structure.

The  $p(e, e'\pi^+)n$  reaction has an important place in our study of the quark-gluon structure of hadrons. This has not changed since our original submissions and has only been reinforced by theoretical progress over the last decade. Indeed, theoretical progress has produced robust yet not experimentally validated calculations. Of particular interest are L/T separated pion cross sections and the pion form factor, especially at larger values of  $Q^2$  where one can study nonperturbative dynamics of QCD while searching for a transition to the perturbative regime. Furthermore, data covering a range in  $t$  at fixed  $Q^2$  are of interest in the validation of using the nucleon's pion cloud (Sullivan process) to access the pion form factor. E12-06-101 (pion form factor) and E12-07-105 (L/T separated cross sections) will provide these data and so important information for our understanding of the reaction mechanism and a benchmark for all models used to calculate the structure of light hadrons.

Since our original proposal submission, there has been a dramatic improvement in the understanding of pion electroproduction data. This has enabled us to optimize and link the E12-06-101 and E12-07-105 experiments, which addresses comments from the PAC30 and PAC32 reports regarding a common run plan, and also allows for extending pion form factor data up to the highest possible momentum transfers achievable at a 12 GeV Jefferson Lab –  $Q^2 \sim 8.5 \text{ GeV}^2$ . The execution of the common run plan starts with the summer 2019 E12-06-101/E12-07-105 low energy run.

## II. SCIENTIFIC MOTIVATION REVIEW

Quantum Chromodynamics (QCD) is the strongly interacting part of the Standard Model. It is ultimately responsible for all of nuclear physics; and yet, almost fifty years after the discovery of gluons and quarks, we are only just beginning to understand how QCD builds the basic bricks of nuclei: neutrons and protons, and the pions that bind them together. QCD is characterized by two emergent phenomena: confinement and dynamical chiral symmetry breaking (DCSB). These have far reaching consequences expressed in the character of the simplest mesons.

The importance of the two approved pion experiments in the overall context is summarized below.

### A. E12-06-101: Pion Form Factor up to $Q^2=6 \text{ GeV}^2$ [1]

This will be the fourth time this experiment has been reviewed by the PAC. In previous reviews (PAC18, PAC30, PAC35), the PAC endorsed the scientific goals of this experiment with its highest ‘A’ rating, and listed it as a flagship and early high-impact goal of the upgraded 12 GeV Jefferson Lab. The requirements of the experiment have greatly influenced the design specifications of the new SHMS spectrometer in Hall C, including small forward angle capability, good angular reproducibility (to control systematic errors in the L/T separation) and sufficient missing mass resolution to cleanly separate  $p(e, e'\pi^+)n$  events from  $p(e, e'\pi^+)n\pi^0$ .

Earlier 6 GeV Jefferson Lab measurements were at the beginning of a new era probing the internal pion structure. Measurements in Hall C by the  $F_\pi$  Collaboration [4, 5] confirmed that with a photon virtuality of  $2.45 \text{ GeV}^2$ , one is still far from the resolution region where the pion behaves like a simple quark/anti-quark pair, *i.e.* far from the “asymptotic” limit. However, this perception is based on the assumption that the asymptotic form of the pion’s valence quark parton distribution amplitude (PDA) is valid at  $Q^2=2.45 \text{ GeV}^2$ . The measured pion form factor is a factor of about three larger than the hard QCD prediction [6]. Modern calculations show that this factor could be explained by using a pion valence quark PDA evaluated at a scale appropriate to the experiment [7]. These calculations are closely tied to the DCSB, and thus confirming these calculations empirically would be a great step towards our understanding of QCD.

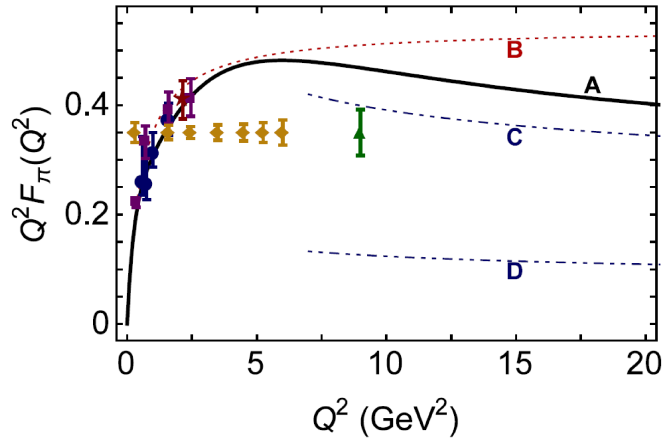


FIG. 1: Existing data (dark blue, purple) and projected uncertainties (yellow, green) for future data on the pion form factor. The solid curve (A) is the QCD-theory prediction bridging large and short distance scales. Curve B is set by the known long-distance scale, the pion radius. Curves C and D illustrate calculations based on a short-distance quark-gluon view. These studies were highlighted in the 2015 NSAC Long Range Plan [9].

The Dyson-Schwinger Equation (DSE) calculations of Ref. [8] indicate one should expect the dominance of hard contributions to the pion form factor for  $Q^2 \geq 8 \text{ GeV}^2$ . At about  $Q^2 \sim 8 \text{ GeV}^2$ , the calculation predicts that  $F_\pi$  will exhibit precisely the momentum-dependence from

QCD, a power law behavior plus logarithmic corrections to scaling, but with the normalization fixed by a pion wave function whose dilation with respect to the asymptotic form is a definite signature of DCSB, which is a crucial feature of the standard model. These studies illustrated in Fig. 1 were recently highlighted in the 2015 NSAC Long Range Plan [9].

The high quality, continuous electron beam of Jefferson Lab, coupled with the recently completed HMS+SHMS system, makes it the only place to seriously pursue a program of  $F_\pi$  measurements. These capabilities provide a unique opportunity that cannot be repeated at foreseeable facilities to extend the pion form factor measurements to  $Q^2=6.0 \text{ GeV}^2$  with high precision, and to  $8.5 \text{ GeV}^2$  with somewhat larger experimental and theoretical uncertainties. The experimental results are expected to serve as an important constraint on the models of the pion GPD. Furthermore, the DSE calculations mentioned above give a direct prediction for the total pion form factor (without separation into soft and hard components), and the proposed data would allow these (and other) calculations to be tested with authority.

### B. E12-07-105: L/T separated pion cross sections to $Q^2=9 \text{ GeV}^2$ [2]

This experiment has been reviewed by two previous PACs. In these reviews (PAC32, PAC38), the PAC endorsed the scientific goal of the experiment to validate the understanding of the hard-exclusive reaction towards 3D imaging. The key to this validation is precision longitudinal-transverse (L/T) separated data. Indeed, the PAC32 report states that “[These data] will provide essential constraints on Generalized Parton Distributions (GPDs) central to the 12 GeV program...even if  $\sigma_T$  is found not to be small...the separation of  $\sigma_L$  may be sufficient for investigating GPDs”. The theory review of PAC38 emphasized that “... the original strong motivation is reinforced by theoretical progress ..., as well as by new ... data”. To date, the need for L/T separated data beyond the 6 GeV regime remains essential. If  $\sigma_T$  is confirmed to be large, it could subsequently allow for a detailed investigation of transversity GPDs. If, on the other hand,  $\sigma_L$  is measured to be larger than expected, this would allow for probing the usual GPDs.

High precision L/T separated data were taken at 6 GeV in Hall C [10] and provided clear evidence for strong contributions from transversely polarized virtual photons. This observation is in sharp contrast to the handbag factorization, which tells us that for asymptotically large  $Q^2$  longitudinally polarized photons dominate [11, 12]. According to the handbag approach, the amplitudes for transverse photons are suppressed  $\sim 1/Q$  as compared to those from longitudinal photons. Unseparated CLAS data [13] are consistent, but must rely on Hall C data for information on individual longitudinal and transverse contributions. For a full review of the strengths of all experimental halls for deep exclusive reactions see the complementarity documentation provided by a working group to PAC40 in 2013 [14]. Additional experimental evidence for strong transverse virtual photon transitions comes from neutral pion electroproduction data from Hall A and B, and the  $\sin \phi_s$  harmonics measured with a transversally polarized target by

HERMES [15].

It has been argued in [16, 17] that, within the handbag approach, the pion electroproduction amplitudes for transversely polarized virtual photons are determined by transversity Generalized Parton Distributions (GPDs), [18, 19]. On the one hand, the amplitudes for transversely polarized photons are parametrically suppressed by  $\mu_\pi/Q$  as compared to the asymptotically leading amplitudes for longitudinally polarized photons (related to the usual GPDs  $\tilde{H}$  and  $\tilde{E}$ ). On the other hand, the parameter  $\mu_\pi$  is fixed by the divergence of the axial-vector current,  $\mu_\pi \approx 2$  GeV (at a scale of 2 GeV). This would suggest that there is no strong suppression of the transverse amplitudes at values of  $Q^2$  accessible in present-day experiments. It is thus of great interest to measure precision longitudinal-transverse separated pion cross sections up to the highest possible value of  $Q^2$ .

In order to evaluate the amplitudes, the transversity GPDs are modeled with the help of the double-distribution ansatz. The pertinent parameters are fixed by fitting the HERMES data on  $\pi^+$  electroproduction and by lattice QCD results [20]. One should bear in mind that these estimates could have uncertainties of about at least a factor of two [21]. In order to determine the transversity GPDs, more precise pion electroproduction data at larger values of  $Q^2$  and  $W$ , than available from JLab at 6 GeV, are needed. A particularly clean probe of large transversity effects in pion electroproduction is the measurement of the relative contribution of  $\sigma_L$  and  $\sigma_T$  to the cross section as a function of  $Q^2$ . The standard handbag approach predicts  $\sigma_L \gg \sigma_T$  while strong transversity effects would lead to  $\sigma_L < \sigma_T$ . Exclusive  $\pi^+$  electroproduction cross sections with L/T separation could confirm the large contribution from transversely polarized photons to this process and may subsequently allow for a detailed investigation of transversity GPDs [21]. Conversely, the separated longitudinal cross section could allow for probing the usual GPDs through pion production.

A large acceptance device like CLAS12 is well suited for measuring pseudoscalar meson electroproduction over a large range of  $-t$  and  $x_B$ . The large azimuthal coverage allows a good determination of the interference terms, but the error amplification in the extraction of longitudinal and transverse components of the cross section (see section V) is a major constraint. In addition, the rates for the listed kinematic points would decrease significantly due to the lower luminosity in Hall B. E12-07-105 will thus use the SHMS and HMS in Hall C as their characteristics best address the experimental requirements.

### III. OPTIMIZATION OF TWO EXPERIMENTS INTO ONE PROGRAM

Experimental studies over the last decade have given us confidence in the reliability of separating  $\sigma_L$  from  $\sigma_T$  (and LT, TT) through the Rosenbluth method. The method entails measuring the cross section at two beam energies and fixed  $W$ ,  $Q^2$ , and  $-t$  and a simultaneous fit using the measured azimuthal angle. Furthermore, for precision cross section measurements a

careful evaluation of the systematic uncertainty is mandatory due to a  $1/\epsilon$  amplification<sup>1</sup> in the  $\sigma_L$  extraction. We propose to make a coincidence measurement between charged pions in the SHMS and electrons in the HMS. A high luminosity spectrometer system like the SHMS+HMS combination in Hall C is well suited for such a measurement. The focusing magnetic spectrometers benefit from small point-to-point uncertainties, which are crucial for meaningful L-T separations. Focusing magnetic spectrometers benefit from small point-to-point uncertainties and are a must for such measurements as excellent control of spectrometer acceptance, kinematics, and efficiencies is required. Both E12-06-101 and E12-07-105 share these stringent requirements and are thus only possible in Hall C.

Pion form factor extractions from E12-06-101 or E12-07-105 L/T separated electroproduction data have additional requirements. Experimental studies over the last decade have given us confidence in the reliability of the electroproduction method yielding the physical pion form factor. We have gained extensive experience during our previous  $F_\pi$  measurements in Hall C [5], as well as lessons learned from previous work at Cornell [22] and DESY [23], and many of the experimental difficulties in extracting the pion form factor at higher  $Q^2$  are now well understood. Our studies included checking the consistency of the model used to extract the form factor from electroproduction data, by extracting the form factor at two values of  $t_{min}$  for fixed  $Q^2$  and verifying that the pole diagram is the dominant contribution to the reaction mechanism. An example is illustrated in Fig. 2. Additional details can be found in section III A, section III B, and section III C.

The resulting  $F_\pi$  values agree to 4% and do not depend on the  $t$  acceptance, which lends confidence in the applicability of the model to the kinematic regime of the data and the validity of the extracted  $F_\pi$  values. The dominance of the  $t$ -channel process in  $\sigma_L$  was verified through the charged pion longitudinal cross section ratios,  $R_L = \sigma_L[n(e, e'\pi^-)p] / \sigma_L[p(e, e'\pi^+)n]$ , obtained with a deuterium target [24]. The data show that  $R_L$  approaches the pion charge ratio, consistent with pion-pole dominance.

This allows for an optimization of the kinematics of the two approved  $p(e, e'\pi^+)n$  experiments to achieve a reliable  $F_\pi$  extraction up to the highest  $Q^2$ , along with similar experimental studies to confirm the results.

In summary, the optimization of the E12-06-101 and E12-07-105 kinematics created a JLab 12 GeV pion precision L/T cross section and Form Factor program featuring:

- Reliable  $F_\pi$  extractions from existing data to the highest possible  $Q^2$
- Validation of  $F_\pi$  extractions at the highest  $Q^2$
- Separated cross sections as function of  $Q^2$  at fixed  $x=0.3, 0.4, 0.55$  to validate the reaction mechanism towards 3D imaging studies

---

<sup>1</sup>  $\Delta\epsilon$  ranges from  $<0.1$  to  $0.3$  in typical exclusive kinematics

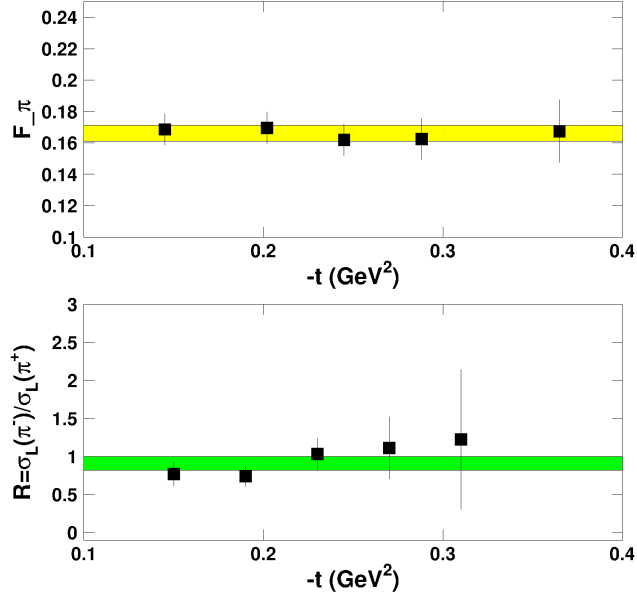


FIG. 2: **Upper panel:** Checking  $t$ - and model-dependence in the pion for factor extraction at a central value of  $Q^2=2.45$  GeV<sup>2</sup> and center-of-mass energy  $W=2.22$  GeV: the solid squares denote the  $F_\pi$  values for the case in which the model was fit to each point separately and the band shows the  $F_\pi$  value obtained from a fit to all points. The error bars and the error band include statistical and uncorrelated uncertainties. **Lower panel:** Checking the dominance of the  $t$ -channel process in  $\sigma_L$  through the charged-pion longitudinal cross section ratios at  $Q^2=2.45$  GeV<sup>2</sup> and  $W=2.22$  GeV. The cross-section ratios are close to unity and much larger than the ratios typically found for the transverse cross section, which is close to  $1/4$ . This significant difference suggests pion pole dominance in the longitudinal cross sections (and parton model dominance in the transverse). The error bars include statistical and uncorrelated uncertainties, and the (green) band denotes the uncertainty of a constant fit to all data points.

The optimized program also addresses several points raised by the previous PACs as detailed in section IV. Fig. 3 summarizes the optimized kinematics as a function of  $Q^2$  and  $W$  (which may be viewed as another way to express  $-t_{min}$ ) up to the highest possible value of  $Q^2$ .

### A. The role of the proton's pion cloud

The electron deep-inelastic-scattering off the meson cloud of a nucleon target is called the Sullivan process. The Sullivan process can provide reliable access to a meson target as  $t$  becomes space-like if the pole associated with the ground-state meson ( $t$ -pole) remains the dominant feature of the process and the structure of the related correlation evolves slowly and smoothly with virtuality. The E12-06-101 and E12-07-105 program will provide data covering a range in  $-t$ , particularly low  $-t$ , to check if these conditions are satisfied empirically, and compare with phenomenological and theoretical expectations. Theoretically, a recent calculation [25] explored

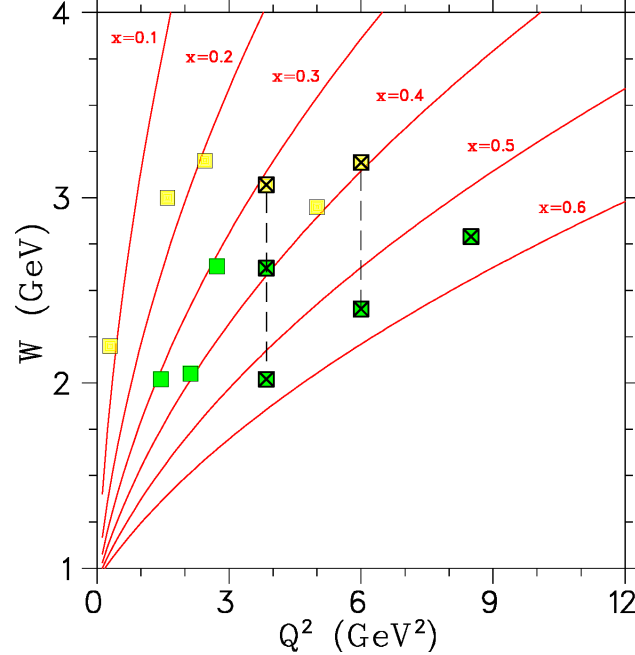


FIG. 3: Updated  $W$  versus  $Q^2$  settings planned for the  $F_\pi$  experiment (yellow squares) and the “Pion Scaling” experiment E12-07-105 (green squares). The points instrumental in the higher  $Q^2$   $F_\pi$  extraction are indicated with ‘X’. The red lines indicate fixed  $x$  values from 0.1 to 0.6. The dashed lines denote scans in  $t$  at fixed  $Q^2$ , which will be used to evaluate the dependence of the  $F_\pi$  extraction on  $t$  as shown in Fig. 2.

the circumstances under which these conditions should be satisfied and found to  $-t \leq 0.6 \text{ GeV}^2$ , all changes in pion structure are modest so that a well-constrained experimental analysis should be reliable.

The experimental determination of the pion form factor from low  $-t$  electroproduction data, the interpretability issues which affected the high  $Q^2$  data from Cornell, and how these issues may be controlled, are explained at length in our 2006 proposal [1]. To briefly summarize, L/T-separated  $p(e, e'\pi^+)n$  cross sections versus  $t$  over some range of  $Q^2$  and  $W$  are the actual observables measured by the experiment, and the extraction of the pion form factor from these data is via a phenomenological model. Our 4–6 GeV measurements in Hall C have shown this approach to yield reliable  $F_\pi$  values from forward kinematics data [5]. Since the VGL Regge model [26] is able, without fitted parameters, to provide a good description of both  $\pi^+$  and  $\pi^-$  photoproduction data, and of  $\sigma_L$  electroproduction data over a range in  $W$ ,  $t$ , and  $Q^2$ , we have used it to extract pion form factor values from the JLab  $\sigma_L$  data up to a maximum  $Q^2$  value of  $2.45 \text{ GeV}^2$ .

Ideally, one would like to have a variety of reliable electroproduction models to choose from, so that the model dependence of the extracted  $F_\pi$  values can be better understood. The anticipated data from this experiment has provided much motivation for phenomenological model building of the  $p(e, e'\pi^+)n$  reaction: Kaskulov & Mosel [27], Goloskokov & Kroll [28], Vrancx &

Ryckebusch [29], Choi, Kong & Yu [30], and Perry, Kizilersu & Thomas [31]. Since it remains our intent to publish the  $\sigma_L$  values obtained by our experiment, other  $F_\pi$  values may result when better models become available in the future.

It is important to note that for  $W$  above the resonance region, the  $t$ -channel pion pole process dominates  $\sigma_L$  for small  $-t$  and contributes unequally to the L, T, TT, and LT responses. Competing non-pole production processes also contribute to  $\sigma_L$ , but they are small in forward kinematics (*i.e.*  $-t_{min} < 0.2 \text{ GeV}^2$ ) and do not have a pole at  $t = m_\pi^2$ . To maximize the contribution of the  $t$ -channel process, as well as separate it from the others which tend to disguise its effect, one measures at a low  $-t$  in parallel and near-parallel kinematics, and performs a response function separation. This is the approach that will be followed here. The  $Q^2 = 6 \text{ GeV}^2$  upper bound of the E12-06-101 measurements is partly dictated by the requirement  $-t_{min} < 0.2 \text{ GeV}^2$ , needed to assure the dominance of the pion pole process to  $\sigma_L$ .

However, the 11 GeV electron beam energy and Hall C equipment allow reliable L/T-separations within a reasonable amount of beam-time up to about  $Q^2 \sim 9 \text{ GeV}^2$ , the approved high  $Q^2$  point in experiment E12-07-105. If one can experimentally show independence of  $t$ , this would allow one to measure  $F_\pi$  in Hall C to significantly higher than  $Q^2=6.0 \text{ GeV}^2$ . We optimized kinematics for such a data-driven approach, to acquire the additional data which will aid understanding the non-pion pole contributions to  $\sigma_L$  at higher  $-t$ .

### B. Test $F_\pi$ extractions at same $Q^2$ but different $-t_{min}$

In our two previous experiments, E93-021 (Fpi-1) and E01-004 (Fpi-2), we acquired  $p(e, e'\pi^+)n$  L/T-separated  $Q^2 = 1.6 \text{ GeV}^2$  data at different distances from the pion pole and compared the resulting  $F_\pi$  values [5]. Fpi-1 measurements were obtained at  $W = 1.95 \text{ GeV}$ ,  $-t_{min} = 0.152 \text{ GeV}^2$ , while the Fpi-2 data were obtained 35% closer to the pole, at  $W = 2.22 \text{ GeV}$   $-t_{min} = 0.093 \text{ GeV}^2$ . The VGL model incorporates a monopole form for the  $\pi\pi\gamma$  and  $\rho\pi\gamma$  form factors:

$$F_{\pi,\rho}(Q^2) = [1 + Q^2/\Lambda_{\pi,\rho}^2]^{-1}. \quad (1)$$

Apart from the  $\pi\pi\gamma$  and  $\rho\pi\gamma$  form factors, the VGL model is parameter free, as the coupling constants at the vertices (such as  $g_{\rho\pi\gamma}$ ) are well determined by precise studies and analyses in the resonance region. The optimal value of  $\Lambda_\pi^2$  is determined from a fit to each set of  $\sigma_L$  data (it is insensitive to  $\Lambda_\rho^2$ ), yielding the empirical  $F_\pi$  values. A comparison of the  $F_\pi$  values extracted from the data sets in this manner allows for a direct test of the theoretical model dependence. The two  $F_\pi$  values extracted from  $Q^2=1.6 \text{ GeV}^2$  data at  $W=1.95, 2.22 \text{ GeV}$  are in excellent agreement (4% difference, well within errors), suggesting only a small uncertainty due to fitting the VGL model to the  $\sigma_L$  data. This technique is not specifically wedded to the VGL model, in principle any model used to extract  $F_\pi$  from electroproduction data should pass this test.

As part of the validation procedure for the extraction of  $F_\pi$  in our experiments, particularly

the higher  $-t$   $Q^2=8.5$  GeV<sup>2</sup> data, we will perform several similar tests. At  $Q^2=3.85$  GeV<sup>2</sup>, we will acquire three sets of L/T-separated data, at  $-t=0.120$  GeV<sup>2</sup>,  $W=3.07$  GeV;  $-t=0.208$  GeV<sup>2</sup>,  $W=2.62$  GeV; and  $-t=0.487$  GeV<sup>2</sup>,  $W=2.02$  GeV. We will extract  $F_\pi$  from all three sets of data and see if they are consistent. A second test will be performed at higher  $Q^2=6.00$  GeV<sup>2</sup>, at  $-t=0.214$  GeV<sup>2</sup>,  $W=3.19$ ; and  $-t=0.530$  GeV<sup>2</sup>,  $W=2.40$  GeV. If the two  $F_\pi$  values extracted from these higher  $Q^2$  data are consistent, then we will have very good reason to believe that our extraction of  $F_\pi$  is reliable. If they are not initially consistent, then the redundant scans are absolutely vital for understanding the nature of the non-pole backgrounds, so that  $F_\pi$  can ultimately be extracted from the data.

### C. The sensitivity of $\pi^-/\pi^+$ measurements to non-pion pole backgrounds

An important tool to infer the presence of isoscalar backgrounds to  $\sigma_L$  is the measurement of the ratio

$$R_L = \frac{\sigma(n(e, e'\pi^-)p)}{\sigma(p(e, e'\pi^+)n)} = \frac{|A_v - A_s|^2}{|A_v + A_s|^2}$$

using a liquid deuterium target. The  $t$ -channel pion-pole diagram is a purely isovector process, and so at small  $-t$ ,  $R_L$  should be near unity. Isoscalar backgrounds are expected to be suppressed by the  $\sigma_L$  response function extraction. Nonetheless, if they are present to any significant degree, they will result in a dilution of the ratio.  $R_L$  data were acquired as part of our Fpi-1, Fpi-2 experiments, and proved themselves to be extremely valuable in two ways:

1. In Fpi-2, the extraction of  $F_\pi$  from our  $Q^2=1.6, 2.45$  GeV<sup>2</sup>,  $W=2.2$  GeV data via the VGL model encountered no significant difficulties. We estimated only a small model dependence in the  $F_\pi$  results, and the  $R_L$  data confirmed that isoscalar backgrounds in these data were small.
2. In Fpi-1, we encountered inconsistencies when extracting  $F_\pi$  from our  $Q^2=0.6-1.6$  GeV<sup>2</sup>,  $W=1.95$  GeV data. We were required to apply corrections to the VGL model and assess a larger model dependence.  $R_L$  data not only confirmed the presence of isoscalar contributions to our higher  $-t$  data, but they also indicated that these contributions are much smaller near  $-t_{min}$ , validating the approach we followed to extract  $F_\pi$  from these data.

The comparison of these two sets of results is shown in more detail Fig. 4. The top row shows the values of  $\Lambda_\pi^2$  determined from fits of the VGL model to our  $\sigma_L$  data. The bottom row shows the  $R_L$  data for the same settings. In the right column are our  $Q^2=2.45$  GeV<sup>2</sup>,  $W=2.2$  GeV data, where neither the  $\Lambda_\pi^2$  nor  $R_L$  values display any statistically significant  $t$ -dependence, indicating the dominance of the  $t$ -channel diagram across the full range of the data. In this case, the  $R_L$  data confirmed that it was possible to extract  $F_\pi$  from the  $\sigma_L$  data without further

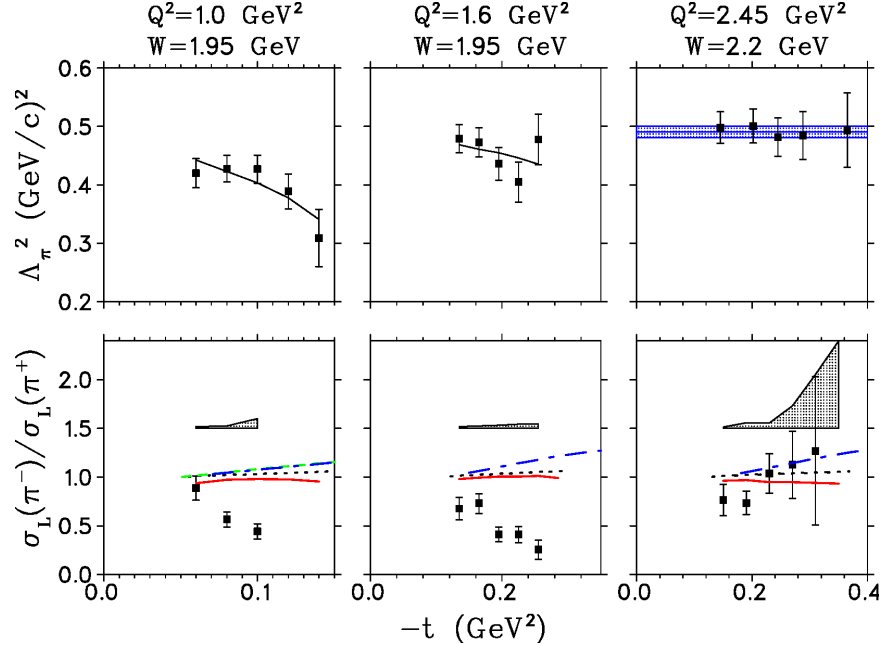


FIG. 4: **Top Row:** Consistency check for the extraction of  $F_\pi$  from Fpi-1, Fpi-2 data by plotting the value of  $\Lambda_\pi^2$  determined from the fit of the VGL model to each  $t$ -bin of  $\sigma_L$  data. If the  $\Lambda_\pi^2$  values display no  $t$ -dependence, no further corrections are needed to extract  $F_\pi$  from the data, as indicated in the right-most  $W=2.2$  GeV panel. The left and center panels required additional corrections and model-dependence, as discussed in Ref. [5]. **Bottom Row:**  $R_L$  data compared to a variety of models (e.g. dotted black [26]; dot-dashed blue [29]).  $R_L \sim 0.8$ , near  $-t_{\min}$  at each  $Q^2$  setting, corresponding to  $A_S/A_V = 6\%$  under the not necessarily realistic assumption that the isoscalar and isovector amplitudes are real. At higher  $-t$ , the  $W=1.95$  GeV  $R_L$  data deviate strongly from both this ratio and the expectations of various models, indicating the presence of isoscalar contributions to  $\sigma_L$ . For more details see Ref. [32].

corrections. The situation is somewhat different for the  $Q^2=1.0, 1.6$  GeV<sup>2</sup> data at  $W=1.95$  GeV (left and center columns).  $\Lambda_\pi^2$  drops at higher  $-t$  due to additional contributions to  $\sigma_L$  not taken into account by the VGL model. The  $R_L \sim 0.8$  values near  $-t_{\min}$  indicate that the non-pole contributions are small there, but the dropping  $R_L$  values indicate they grow rapidly at higher  $-t$ . In these cases, the  $R_L$  data validate the approach we used to extract  $F_\pi$  from these data, which relied on the assumption that non-pole contributions were smallest at  $-t_{\min}$ . The bottom line is that  $R_L$  tests can and must be performed to indicate where the longitudinal data are dominated by the  $t$ -channel process. This lends confidence in the  $F_\pi$  values extracted from the experimental data.

Unfortunately, it is experimentally expensive to carry out these  $\pi^-/\pi^+$  measurements. Due to the negative polarity of the pion spectrometer, electron singles rates are high and it is usually necessary to lower the beam current from about 70  $\mu\text{A}$  to 10-15  $\mu\text{A}$  to maintain the excellent tracking and particle identification needed for reliable L/T-separations. We have reorganized our planned settings to enable  $\pi^-/\pi^+$  data to be acquired at intermediate  $-t_{\min}$ ,

so that the evolution of the non-pole backgrounds versus  $-t$  can be better understood. The revised  $\pi^-/\pi^+$  plan includes scans at  $Q^2=3.85$  GeV<sup>2</sup>,  $W=3.07$  GeV,  $-t_{min}=0.120$  GeV<sup>2</sup> and  $Q^2=3.85$  GeV<sup>2</sup>,  $W=2.62$  GeV,  $-t_{min}=0.208$  GeV<sup>2</sup>. We have also investigated whether it would be feasible to acquire  $\pi^-/\pi^+$  measurements at  $Q^2=8.5$  GeV<sup>2</sup>,  $W=2.79$  GeV,  $-t_{min}=0.550$  GeV<sup>2</sup>, but this would take a prohibitive 3600 PAC-hrs of beam. Therefore, we have reoptimized the kinematics of E12-07-105 to perform this test at  $Q^2=6.0$  GeV<sup>2</sup>,  $W=2.40$  GeV,  $-t_{min}=0.530$  GeV<sup>2</sup>, where the pion production cross sections and electron singles rates are projected to be much more favorable. Since the  $-t$  and  $Q^2$  values are similar, and our previous  $R_L$  measurements indicate only a weak  $Q^2$ -dependence at fixed  $-t$ , we believe this measurement will provide vital information on any non-pole backgrounds contributing to  $\sigma_L$  at  $Q^2=8.5$  GeV<sup>2</sup>. These  $\pi^-/\pi^+$  data are vital to determine the presence of non-pole backgrounds if  $F_\pi$  is to be reliably extracted from higher  $-t$  electroproduction data.

#### IV. COMPREHENSIVE KINEMATICS PLAN

The optimized kinematics for both E12-06-101 and E12-07-105 are presented graphically in Fig. 3 and in detail in Tables I, II. A detailed running-time breakdown in comparison to our previous PAC approval is shown in Table III. The total time to do the combined program fits within the total PAC-approved allocation.

In the optimization of the two experiments, we took into account the comments of the PAC30 [33] and PAC32 [34] written reports.

- Justification of the beam time for the highest  $x/Q^2$  point (PAC32):
  - We moved the previous E12-07-105 point at  $Q^2=9.1$  GeV<sup>2</sup> to  $Q^2=8.5$  GeV<sup>2</sup> to extend pion form factor data to the highest possible  $Q^2$  at the 12 GeV Jefferson Lab. This setting benefits from reduced uncertainties due to higher rate and more favorable  $1/\Delta\epsilon$  error magnification. Some beam time was added for the higher statistics needed for the  $F_\pi$  extraction. Overall, the potential physics outcome fully justifies the large beam time requirement.
  - The  $Q^2=8.5$  GeV<sup>2</sup> setting requires non-standard beam energies. If only standard beam energies are required, our run plan can be adjusted to a highest  $Q^2$  of 8.3 GeV<sup>2</sup>.
- Optimization between the two experiments (PAC32):
  - To achieve better overlap between the two experiments, we moved the  $Q^2=6.6$  GeV<sup>2</sup> point from E12-07-105 to 6.0 GeV<sup>2</sup>. Together with the E12-06-101 point at  $Q^2=6.0$  GeV<sup>2</sup>, this provides a suitable range from  $-t=0.21$  to  $-t=0.80$  GeV<sup>2</sup>, to verify the reliability of  $F_\pi$  extraction at higher  $Q^2$  and higher  $-t$ .

TABLE I: Optimized settings for the E12-06-101 (Fpi-12) experiment. The scattered electron will be detected in the HMS and the pion in the SHMS. LH+, LD+, LD- indicate the combination of cryotarget type and SHMS (pion) polarity. Hours per setting include both full and dummy target data taking, as well as 4 hours of overhead. The settings in *blue italics* are used for both the pion form factor and pion scaling studies. The settings in *red* are scheduled to run in the summer of 2019, and have been adjusted to reflect scheduled beam energies and spectrometer angles.

$Q^2$	$W$	$x$	$-t_{min}$	Type	$E_e$	$\epsilon$	$\theta_q$	$\theta_{\pi q}$	Hrs
<i>0.38</i>	<i>2.20</i>	<i>0.087</i>	<i>0.008</i>	LH+	<i>2.8</i>	<i>0.286</i>	<i>5.70</i>	<i>0, +2, +4°</i>	<i>11.1</i>
					<i>3.7</i>	<i>0.629</i>	<i>8.87</i>	<i>-2, 0, +2, +4°</i>	<i>14.8</i>
					<i>4.6</i>	<i>0.781</i>	<i>10.33</i>	<i>-4, -2, 0, +2, +4°</i>	<i>18.5</i>
1.60	3.00	0.165	0.029	LH+	6.7	0.408	6.36	0, +2°	9.9
					8.8	0.689	8.70	-2, 0, +2°	12.8
					11.0	0.817	9.91	-2, 0, +2°	12.8
1.60	3.00	0.165	0.029	LD+	6.7	0.408	6.36	0, +2°	9.9
					11.0	0.817	9.91	-2, 0, +2°	12.8
1.60	3.00	0.165	0.029	LD-	6.7	0.408	6.36	0, +2°	18.7
					11.0	0.817	9.91	-2, 0, +2°	12.8
2.45	3.20	0.208	0.048	LH+	8.0	0.383	6.26	0, +2°	9.9
					8.8	0.505	7.30	-1.8, 0, +2°	12.8
					11.0	0.709	9.03	-2, 0, +2°	12.8
<i>3.85</i>	<i>3.07</i>	<i>0.311</i>	<i>0.120</i>	LH+	<i>8.0</i>	<i>0.301</i>	<i>6.53</i>	<i>-1.03, 0, +2°</i>	<i>33.5</i>
					<i>8.8</i>	<i>0.436</i>	<i>7.97</i>	<i>-2, 0, +2°</i>	<i>18.2</i>
					<i>9.9</i>	<i>0.572</i>	<i>9.31</i>	<i>-2, 0, +2°</i>	<i>13.3</i>
					<i>11.0</i>	<i>0.666</i>	<i>10.27</i>	<i>-2, 0, +2°</i>	<i>12.8</i>
3.85	3.07	0.311	0.120	LD+	8.0	0.301	6.53	-1.03, 0, +2°	33.5
					11.0	0.666	10.27	-2, 0, +2°	12.8
3.85	3.07	0.311	0.120	LD-	8.0	0.301	6.53	0, +2°	118.8
					11.0	0.666	10.27	-2, 0, +2°	12.8
<i>5.00</i>	<i>2.95</i>	<i>0.390</i>	<i>0.209</i>	LH+	<i>8.0</i>	<i>0.238</i>	<i>6.35</i>	<i>0, +2°</i>	<i>74.5</i>
					<i>9.9</i>	<i>0.530</i>	<i>9.76</i>	<i>-2, 0, +2°</i>	<i>41.1</i>
					<i>11.0</i>	<i>0.633</i>	<i>10.88</i>	<i>-2, 0, +2°</i>	<i>27.0</i>
<i>6.00</i>	<i>3.19</i>	<i>0.392</i>	<i>0.214</i>	LH+	<i>9.2</i>	<i>0.184</i>	<i>5.13</i>	<i>0.37, +2°</i>	<i>182.2</i>
					<i>9.9</i>	<i>0.304</i>	<i>6.64</i>	<i>0, +2°</i>	<i>80.6</i>
					<i>11.0</i>	<i>0.452</i>	<i>8.22</i>	<i>-2, 0, +2°</i>	<i>71.9</i>
Calibrations									80.0
Beam Energy Changes									72.0
Total Hours (100% efficiency)									1054.6
PAC35 Approved Hours (100% efficiency)									1248.0
Time Saved: 1248-1054.6 hrs (100% efficiency)									-193.4

- The approved intermediate  $Q^2$  points from both E12-06-101 and E12-07-105 were rearranged to a common  $Q^2=3.85$  GeV<sup>2</sup>, to better investigate the  $t$ -dependence of the reaction. These points also included measurements of the  $\pi^+/\pi^-$  ratio, which will allow us to test for QCD backgrounds in the  $F_\pi$  extraction.

- Optimization of the schedule (PAC30):

- Considerable time was saved by eliminating points at  $Q^2=4.46$  GeV<sup>2</sup> (E12-06-101)

TABLE II: Optimized settings for the E12-07-105 (Pion Scaling) experiment, as per Table I. The settings in **bold face** are for the pion form factor extraction at high  $Q^2$ . The settings in *blue italics* are for validating the possibility of pion form factor extractions at high  $-t$  at  $Q^2=3.85$  GeV<sup>2</sup>. The settings in **red** are scheduled to run in the summer of 2019.

$Q^2$	$W$	$x$	$-t_{min}$	Type	$E_e$	$\epsilon$	$\theta_q$	$\theta_{\pi q}$	Hrs
1.45	2.02	0.312	0.114	LH+	<b>3.7</b>	<b>0.511</b>	<b>13.76</b>	<b>-2, 0, +2°</b>	<b>11.1</b>
					6.7	0.880	20.17	-2, 0, +2°	10.0
2.73	2.63	0.311	0.118	LH+	6.7	0.513	10.30	-2, 0, +2°	13.8
					11.0	0.845	14.58	-2, 0, +2°	9.3
2.12	2.05	0.390	0.195	LH+	<b>4.6</b>	<b>0.573</b>	<b>15.14</b>	<b>-2, 0, +2°</b>	<b>11.1</b>
					8.8	0.907	21.44	-2, 0, +2°	12.8
3.85	2.62	0.392	0.208	LH+	6.7	0.360	8.94	-2, 0, +2°	22.5
					11.0	0.799	14.58	-2, 0, +2°	9.6
<i>3.85</i>	<i>2.62</i>	<i>0.392</i>	<i>0.208</i>	<i>LD+</i>	<i>6.7</i>	<i>0.360</i>	<i>8.94</i>	<i>-2, 0, +2°</i>	<i>22.5</i>
					<i>11.0</i>	<i>0.799</i>	<i>14.58</i>	<i>-2, 0, +2°</i>	<i>9.6</i>
<i>3.85</i>	<i>2.62</i>	<i>0.392</i>	<i>0.208</i>	<i>LD-</i>	<i>6.7</i>	<i>0.360</i>	<i>8.94</i>	<i>-2, 0, +2°</i>	<i>74.9</i>
					<i>11.0</i>	<i>0.799</i>	<i>14.58</i>	<i>-2, 0, +2°</i>	<i>9.6</i>
3.85	2.02	0.546	0.487	LH+	6.0	0.582	17.41	-2, 0, +2°	9.6
					11.0	0.898	21.92	-2, 0, +2°	9.6
6.00	2.40	0.551	0.530	LH+	8.0	0.449	11.26	-2, 0, +2°	48.5
					11.0	0.738	15.31	-2, 0, +2°	18.4
<i>6.00</i>	<i>2.40</i>	<i>0.551</i>	<i>0.530</i>	<i>LD+</i>	<i>8.0</i>	<i>0.449</i>	<i>11.26</i>	<i>-2, 0, +2°</i>	<i>48.5</i>
					<i>11.0</i>	<i>0.738</i>	<i>15.31</i>	<i>-2, 0, +2°</i>	<i>18.4</i>
<i>6.00</i>	<i>2.40</i>	<i>0.551</i>	<i>0.530</i>	<i>LD-</i>	<i>8.0</i>	<i>0.449</i>	<i>11.26</i>	<i>-2, 0, +2°</i>	<i>48.5</i>
					<i>11.0</i>	<i>0.738</i>	<i>15.21</i>	<i>-2, 0, +2°</i>	<i>18.4</i>
<b>8.50</b>	<b>2.79</b>	<b>0.552</b>	<b>0.550</b>	<b>LH+</b>	<b>9.2</b>	<b>0.156</b>	<b>5.52</b>	<b>0°</b>	<b>388.0</b>
					<b>11.0</b>	<b>0.430</b>	<b>9.36</b>	<b>0°</b>	<b>108.5</b>
Calibrations									48.0
Extra calibrations needed for large angle $y_{tar}$									8.0
Beam energy changes									72.0
Total Hours (100% efficiency)									1057.3
PAC38 Approved Hours (100% efficiency)									864.0
Extra time: 1035.3-864.0 (Table I) hrs (100% efficiency)									+193.5

and  $Q^2=5.50$  GeV<sup>2</sup> (E12-07-105). The  $Q^2=5.25$  GeV<sup>2</sup> point of E12-06-101 was moved to  $Q^2=5.00$  GeV<sup>2</sup>, so that it may serve double-duty as part of the  $x=0.39$  scan of E12-07-105.

- Where possible, we revised all settings to minimize the number of settings requiring special linac gradients, and reduce the most forward SHMS angle requirements. Rates are based on a SIMC Monte Carlo simulation using the VR cross-section model [29], with all experimental acceptance and missing mass cuts applied.
- Use of a 10-cm long target to reduce the beam current (PAC30):
  - We have increased the target cell length from 8 cm to 10 cm. This allows for a reduction of the maximum beam current from 85  $\mu$ A (with 8 cm target as assumed for PAC35/38) to 70  $\mu$ A.

TABLE III: Detailed breakdown of optimized run times compared to PAC35 and PAC38 approvals.

$Q^2$	$W$	$x$	$-t_{min}$	Type	PAC35	New Plan	Difference (New-PAC35)
E12-06-101 (Fpi-12)							
0.38	2.20	0.070	0.005	LH+	36	44.4	
1.60	3.00	0.165	0.029	LH+	36	35.5	
				LD+	20	22.7	
				LD-	25	31.5	
2.45	3.20	0.208	0.048	LH+	57	35.5	-4.4
3.50	3.10	0.286	0.099	LH+	48		
				LD+	32		
				LD-	157		
3.85	3.07	0.311	0.120	LH+		77.8	
				LD+		46.3	
				LD-		131.6	18.7
4.46	3.25	0.315	0.124	LH+	122		
5.25	3.20	0.359	0.171	LH+	216		
5.00	2.95	0.390	0.209	LH+		142.6	-195.4
6.00	3.19	0.392	0.214	LH+	345	334.7	-10.3

$Q^2$	$W$	$x$	$-t_{min}$	Type	PAC38	New Plan	Difference (New-PAC38)
E12-07-105 (Pion Scaling)							
1.45	2.02	0.312	0.114	LH+	9.4	21.1	
2.73	2.63	0.311	0.118	LH+	14.4	23.0	
4.00	3.12	0.311	0.120	LH+	14.1		5.2
2.12	2.05	0.390	0.195	LH+	9.6	20.3	
				LD-	9.6		1.1
3.85	2.62	0.392	0.208	LH+		32.1	
				LD+		32.1	
				LD-		84.5	
4.00	2.67	0.390	0.206	LH+	23.5		
				LD+			
				LD-	23.5		101.7
5.50	3.08	0.390	0.210	LH+	38.6		
				LD+			
				LD-	38.6		-77.2
3.85	2.02	0.546	0.487	LH+		19.2	
4.00	2.04	0.549	0.498	LH+	14.6		4.6
6.60	2.51	0.549	0.530	LH+	152.8		
6.00	2.40	0.551	0.530	LH+		66.9	-85.9
6.00	2.40	0.551	0.530	LD+		66.9	
				LD-		66.9	133.8
8.50	2.79	0.552	0.550	LH+		496.5	
9.10	2.89	0.549	0.545	LH+	416.4		80.1

- Precise L/T separations require a systematic understanding of the spectrometer acceptance over the extended target length. The largest target is with the HMS spectrometer at 57 degrees. We have added 8 hours to allow for detailed checks of the acceptance in Table II.

To ensure the reliability of the potentially high impact  $Q^2=8.5$  GeV<sup>2</sup> pion form factor

measurement, we added some additional studies of the possible non-pole contributions in Table II. Specifically, a new set of  $\pi^-/\pi^+$  measurements was added at  $Q^2=6.0 \text{ GeV}^2$ , at comparable  $-t$  to the  $Q^2=8.5 \text{ GeV}^2$   $F_\pi$  extraction point. Since our previous  $R_L$  measurements indicate only a weak  $Q^2$ -dependence at fixed  $-t$  [32], we expect this measurement to provide vital information on the non-pole backgrounds contributing to  $\sigma_L$  at  $Q^2=8.5 \text{ GeV}^2$ .

It should also be noted that in comparison to what was planned for PAC35/38, the SHMS solid angle is now a bit smaller. This has resulted in an increase of beam time for some settings in comparison to PAC35/38, but this is offset by the savings produced by combining other settings.

## V. PROJECTED RESULTS

A minimum of two measurements at fixed  $(Q^2, W)$  and different values of  $\epsilon$  are needed in order to determine  $\sigma_L$ . Thus if  $\sigma_1 = \sigma_T + \epsilon_1\sigma_L$  and  $\sigma_2 = \sigma_T + \epsilon_2\sigma_L$  then

$$\sigma_L = \frac{1}{\epsilon_1 - \epsilon_2}(\sigma_1 - \sigma_2).$$

Assuming uncorrelated errors in the measurement of  $\sigma_1$  and  $\sigma_2$ , we obtain the intermediate expression

$$\frac{\Delta\sigma_L}{\sigma_L} = \frac{1}{(\epsilon_1 - \epsilon_2)} \frac{1}{\sigma_L} \sqrt{\Delta\sigma_1^2 + \Delta\sigma_2^2},$$

and by defining  $r \equiv \sigma_T/\sigma_L$

$$\frac{\Delta\sigma_L}{\sigma_L} = \frac{1}{\epsilon_1 - \epsilon_2} \sqrt{\left(\frac{\Delta\sigma_1}{\sigma_1}\right)^2 (r + \epsilon_1)^2 + \left(\frac{\Delta\sigma_2}{\sigma_2}\right)^2 (r + \epsilon_2)^2}.$$

This useful equation makes explicit the error amplification due to a limited  $\epsilon$  range and (potentially) large  $r$ .

Using the approximation that  $\sigma_L \propto F_\pi^2$ , the experimental error in  $F_\pi$  is

$$\frac{\Delta F_\pi}{F_\pi} = \frac{1}{2} \frac{1}{(\epsilon_1 - \epsilon_2)} \sqrt{\left(\frac{\Delta\sigma_1}{\sigma_1}\right)^2 (r + \epsilon_1)^2 + \left(\frac{\Delta\sigma_2}{\sigma_2}\right)^2 (r + \epsilon_2)^2}.$$

The relevant quantities for the the extraction of the the L/T separated cross sections and the form factor are  $r = \sigma_T/\sigma_L$  and  $\Delta\epsilon$  between the two kinematic settings.

The extraction of  $F_\pi$  from the data requires that the  $t$  dependence of  $\sigma_L$  be compared to the VGL Regge (or other) model. To estimate the uncertainty in  $F_\pi$ , we took into account both the variation of counts across the SHMS+HMS acceptance at both low and high  $\epsilon$  and the variation in the VR model  $r = \sigma_T/\sigma_L$  across the acceptance. This projection is sensitive to the assumption for the ratio  $r = \sigma_T/\sigma_L$  (shown in Table IV), which may be conservative. The resulting projected error bars, including all statistical, systematic, and model fitting uncertainties, are listed in Table IV and displayed in Fig. 6. An example of the projected uncertainties for the  $Q^2$  dependence of

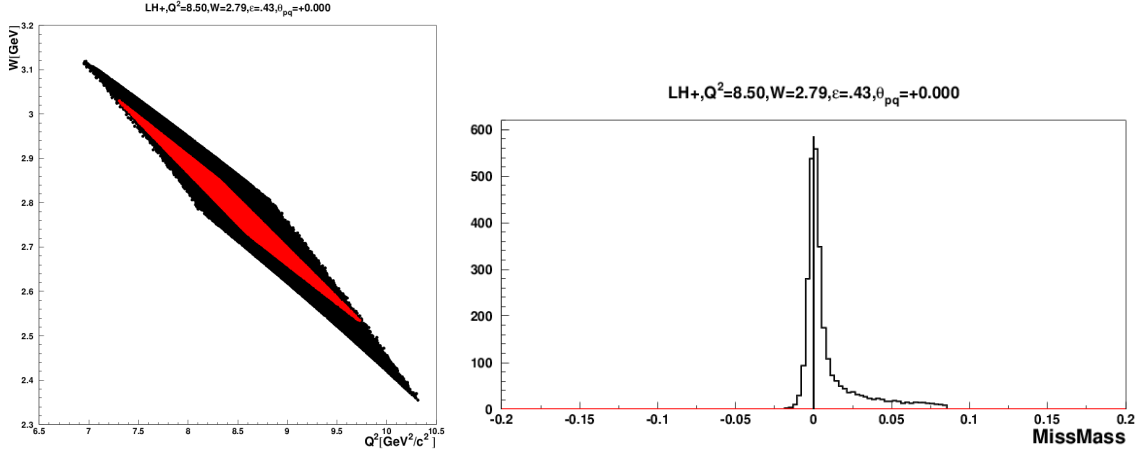


FIG. 5: *Left:* Simulated  $Q^2$  (horizontal axis) versus  $W$  (vertical axis) acceptance for the  $Q^2=8.5$   $\text{GeV}^2$  SHMS+HMS settings. The black points are the acceptance at  $\epsilon=0.430$ , and the red points are the acceptance at  $\epsilon=0.156$ . Cuts are applied to equalize the acceptances of the two settings. **Right:** Simulated  $p(e, e' \pi^+)n$  missing mass distribution for the  $Q^2=8.5$   $\text{GeV}^2$   $\epsilon=0.43$  SHMS+HMS setting (the neutron mass is subtracted). The cutoff at right indicates the limit of the  $0.875 < MM < 1.025$   $\text{GeV}$  cut used for the rate estimates.

TABLE IV: Projected statistical and systematic uncertainties for  $F_\pi(Q^2)$  assuming the VR model cross sections, the  $\epsilon$  values and running times given in Tables I, II and the projected uncertainties given in the E12-06-101 proposal.

$Q^2$ ( $\text{GeV}^2$ )	$-t_{min}$ ( $\text{GeV}^2$ )	$r \equiv \sigma_T/\sigma_L$	$\Delta\epsilon$	$\Delta F_\pi/F_\pi$ (%)
E12-06-101				
0.30	0.005	0.68	0.406	4.9
1.60	0.029	0.36	0.409	4.1
2.45	0.048	0.37	0.326	4.6
3.85	0.120	0.55	0.365	4.7
5.00	0.209	0.78	0.395	5.0
6.00	0.212	0.70	0.268	6.1
Optimized E12-07-105				
8.50	0.544	1.71	0.274	10.2

the  $\pi^+$  longitudinal cross section is illustrated in Figure 7. The uncertainties on the proposed points have been estimated using a parameterization of both longitudinal and transverse cross sections from previous pion production data, assuming an uncorrelated systematic uncertainty of 1.7% in the unseparated cross section, and correlated uncertainties as listed in Table III in our 2007 proposal. The projected uncertainty in the fitting exponent in the  $Q^n$  dependence are listed in Table IV in our 2007 submission.

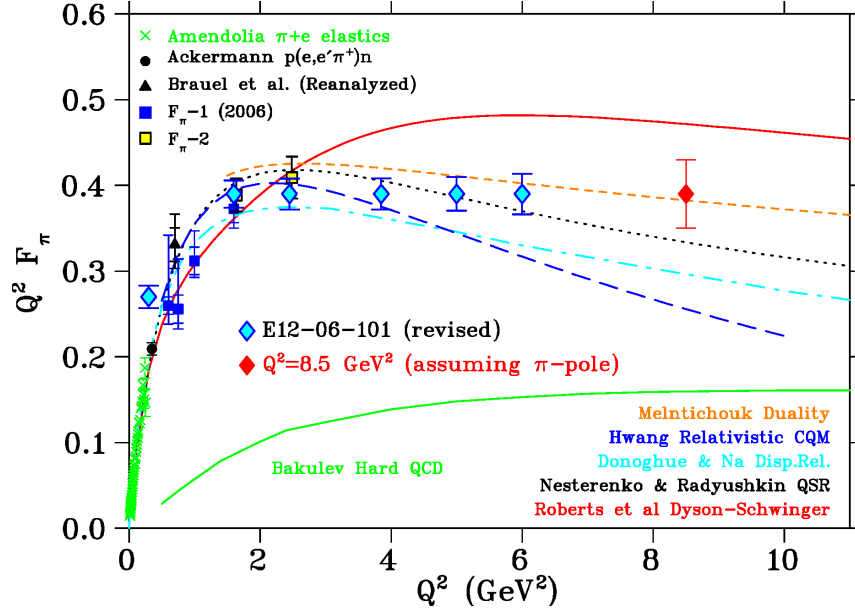


FIG. 6: Projected error bars, in comparison with a variety of theoretical models, and existing precision data. The error bars include all projected statistical and systematic uncertainties.

## VI. SUMMARY

In summary, we request that the PAC confirm the high-impact status of the program we have described in this proposal and maintain the time already approved for the E12-06-101 and E12-07-105 experiments. The combined beam time allocation will:

- enable measurements of the pion form factor at low  $-t_{min}$  up to  $Q^2 = 6 \text{ GeV}^2$
- allow for measurements of the separated  $\pi^+$  cross sections as a function of  $Q^2$  at three fixed  $x$  values, and finally,
- enable the measurement of the pion form factor to the very largest  $Q^2$  accessible at a 12 GeV JLab,  $8.5 \text{ GeV}^2$ .

Since this latter measurement will be at a value of  $-t_{min}$  somewhat larger than that typically used for pion form factor measurements, some time will be used to provide experimental validation of the form factor extraction.

Taken together, this proposal combined with the already approved experiments will provide a comprehensive and coherent program of charged pion electroproduction, separated cross section measurements. Since there are strong theoretical grounds that hard contributions to the pion form factor dominate for  $Q^2 \geq 8 \text{ GeV}^2$  [8], the proposed measurement will contribute greatly to our understanding of the pion form factor in the region where QCD begins to transition from large- to small-distance-scale behavior. Our measurement of  $\sigma_L$  and  $\sigma_T$  plays an important role in the reliable interpretation of the results from the JLab GPD program filling

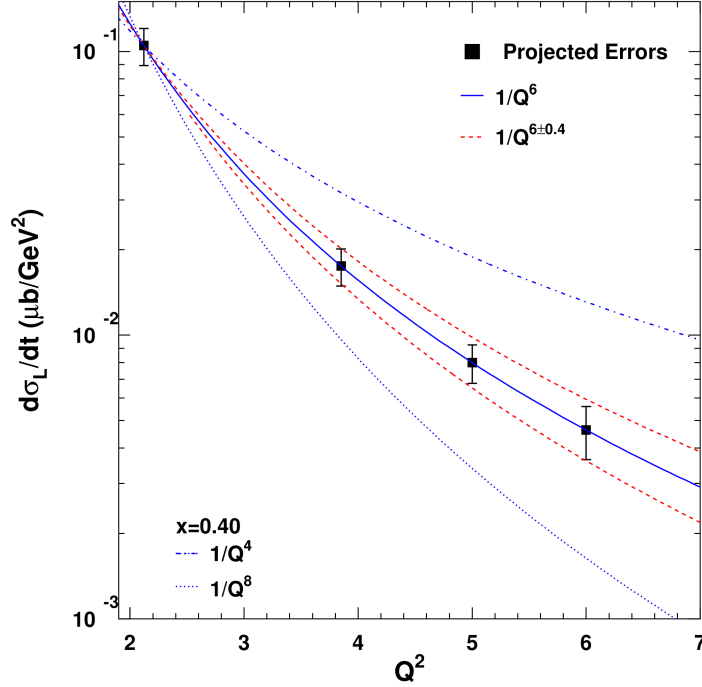


FIG. 7: Projected uncertainties for the  $Q^2$  dependence of  $\sigma_L$  at  $x_B=0.39$ . The data points are plotted to follow  $1/Q^6$  scaling. The uncertainties were determined using a two parameter fit of the form  $A/Q^n$ . The red dashed curves assume a form  $1/Q^n$  for the  $Q^2$  dependence of the longitudinal cross section, and indicates the precision with which one may fit the exponent. The projected uncertainty on  $dn$  depends on the projected uncertainty for  $\sigma_L$ , which in turn depends on  $r=\sigma_L/\sigma_T$ . For consistency with the existing data we have used  $r$  values predicted from our parameterization. If new data suggests that the VGL prediction is more applicable at higher  $Q^2$ , this would reduce the uncertainty on  $dn$  to  $dn=\pm 0.2$ .

an important gap of precision L/T separated  $\pi^+$  data above  $Q^2=2.5$  GeV<sup>2</sup> where theoretical predictions have large uncertainties. If  $\sigma_T$  is confirmed to be large this could subsequently allow for a detailed investigation of transversity GPDs. If, on the other hand,  $\sigma_L$  is measured to be larger than expected, this would allow for probing the usual GPDs. The L/T separated cross sections over a large range in  $-t$  could also aid in verifying if the conditions for the Sullivan process are satisfied empirically.

- 
- [1] G.M. Huber, D.J. Gaskell, et al., Jefferson Lab Experiment E12-06-101, “Measurement of the Charged Pion Form Factor to High  $Q^2$ ”,  
[http://www.jlab.org/exp\\_prog/proposals/06/PR12-06-101.pdf](http://www.jlab.org/exp_prog/proposals/06/PR12-06-101.pdf)
  - [2] T. Horn, G.M. Huber, et al., Jefferson Lab Experiment E12-07-105, “Scaling Study of the L-T Separated Pion Electroproduction Cross Section at 11 GeV”,  
[http://www.jlab.org/exp\\_prog/proposals/07/PR12-07-105.pdf](http://www.jlab.org/exp_prog/proposals/07/PR12-07-105.pdf)
  - [3] T. Horn, C.D. Roberts, Journal of Physics G: Nuclear and Particle Physics, Vol. 43, Issue 7, 073001

- (2016), arXiv:1602.04016.
- [4] T. Horn, et al., Phys. Rev. Lett. **97** (2006) 192001.
  - [5] G.M. Huber, et al., Phys. Rev. C **78** (2008) 045203.
  - [6] A.P. Bakulev, K. Passek-Kumericki, W. Schroers, N.G. Stefanis, Phys. Rev. D **70** (2004) 033014; and erratum **70** (04) 079906.
  - [7] L. Chang, I.C. Cloet, J.J. Cobos-Martinez, C.D. Roberts, S.M. Schmidt, P.C. Tandy, Phys. Rev. Lett. **110** (2013) 132001.
  - [8] L. Chang, I.C. Cloet, C.D. Roberts, S.M. Schmidt, P.C. Tandy, Phys. Rev. Lett. **111** (2013) 141802.
  - [9] Department of Energy, Nuclear Science Advisory Committee, “Reaching for the Horizon” Long Range Plan (2015),  
[https://science.osti.gov/-/media/np/nsac/pdf/2015LRP/2015\\_LRPNS\\_091815.pdf](https://science.osti.gov/-/media/np/nsac/pdf/2015LRP/2015_LRPNS_091815.pdf)
  - [10] T. Horn, et al., Phys. Rev. C **78** (2008) 058201.
  - [11] J.C. Collins, L. Frankfurt, M. Strikman, Phys. Rev. D **56** (1997) 2982.
  - [12] S.J. Brodsky, G.R. Farrar, Phys. Rev. Lett. **31** (1973) 1153.
  - [13] K. Park, et al., Eur.Phys.J. **A49** (2013) 16.
  - [14] M. Pennington, F.X. Girod, M. Guidal, T. Horn, C. Munoz-Camacho, “The Multi-Hall Deep Exclusive Scattering Program at 12 GeV”,  
<https://redmine.jlab.org/attachments/download/805/textmay1.pdf>
  - [15] A. Airapetian, et al., Phys. Lett. **B682** (2010) 345.
  - [16] S.V. Goloskokov and P. Kroll, Eur.Phys.J. **C65** (2010) 137-151.
  - [17] S.V. Goloskokov and P. Kroll, Eur.Phys.J. **A47** (2011) 112.
  - [18] P. Hoodbhoy and X.-D. Ji, Phys. Rev D **58** (1998) 054006.
  - [19] M. Diehl, Eur.Phys.J. **C19** (2001) 485.
  - [20] M. Gockeler, et al., Phys.Lett. **B627** (2005) 113.
  - [21] P. Kroll, Private Communication, 2012.
  - [22] C.J. Bebek, et al., Phys. Rev. D **17** (1978) 1693.
  - [23] P. Brauel, et al., Z. Phys. C **3** (1979) 101.
  - [24] G.M. Huber, et al., Phys. Rev. Lett. **112** (2014) 182501.
  - [25] S.-X. Qin, C. Chen, C. Mezrag and C. D. Roberts, Phys. Rev. C **97** (2018) 015203.
  - [26] M. Vanderhaeghen, M. Guidal, J.-M. Laget, Phys. Rev. C **57** (1997) 1454.  
M. Vanderhaeghen, M. Guidal, J.-M. Laget, Nucl. Phys. **A627** (1997) 645.
  - [27] M.M. Kaskulov, U. Mosel, Phys. Rev. C **81**, 045202 (2010).
  - [28] S. V. Goloskokov and P. Kroll, Eur. Phys. J. **C65**, 137 (2010); Eur. Phys. J. A **47**, 112 (2011).
  - [29] T. Vrancx, J. Ryckebusch, Phys. Rev. C **89**, 025203 (2014).
  - [30] T.K. Choi, K.J. Kong, B.G. Yu, J. Korean Phys. Soc. **67** (2015) L1089, arXiv:1508.00969.
  - [31] R.J. Perry, A. Kizilersu, A.W. Thomas, arXiv:1811.09356, and Private Communication.
  - [32] G.M. Huber, et al., Phys. Rev. C **91** (2015) 015202.
  - [33] Report of the Jefferson Lab Program Advisory Committee - PAC30 (2006),  
[https://www.jlab.org/exp\\_prog/PACpage/PAC30/PAC30\\_report.pdf](https://www.jlab.org/exp_prog/PACpage/PAC30/PAC30_report.pdf)
  - [34] Report of the Jefferson Lab Program Advisory Committee - PAC32 (2007),  
[https://www.jlab.org/exp\\_prog/PACpage/PAC32/PAC32\\_report.pdf](https://www.jlab.org/exp_prog/PACpage/PAC32/PAC32_report.pdf)